



ISSN (Print) : 2320 – 3765  
ISSN (Online): 2278 – 8875

## International Journal of Advanced Research in Electrical, Electronics and Instrumentation Engineering

(An ISO 3297: 2007 Certified Organization)

Website: [www.ijareeie.com](http://www.ijareeie.com)

Vol. 6, Issue 7, July 2017

# Co: Fe<sub>2</sub>O<sub>3</sub>, Co<sub>x</sub>Zn<sub>1-x</sub>Fe<sub>2</sub>O<sub>4</sub> Thin Films Grown by Chemical Spray Pyrolysis for Gas Sensor Application

Sevda S<sup>1</sup>, Mutlu K<sup>1</sup>, Omer C<sup>2</sup>, Muhammet Y<sup>1</sup>

Department of Physics, Ataturk University, 25250, Erzurum, Turkey<sup>1</sup>

Department of Electrical and Energy, Ispir Hamza Polat Vocational School of Higher Education, Ataturk University,  
25250, Erzurum, Turkey<sup>2</sup>

**ABSTRACT:** Air pollution caused by toxic, flammable and explosive gases, detection of some hazardous gases is impossible for human, because some gases like CO and H<sub>2</sub> are odourless and tasteless as well as colourless. Furthermore in some cases absolute gas concentrations is very low to be detected by human nose. Therefore development and fabrication of a device for early detection of certain flammable, explosive, and toxic gases are extremely necessary. For this purpose, different devices have been developed toward tract detection of such pollution gases. Consequently, the development of cheap and reliable devices for detection of gases is considered to be a significant goal in science. In this study, iron oxide compound triple and quaternary iron oxide compounds with Zn, Co metal dopants were grown by using Chemical Spray Pyrolysis (CSP) technique. The structural, optical, magnetic properties of Co:Fe<sub>2</sub>O<sub>3</sub>, Co<sub>x</sub>Zn<sub>1-x</sub>Fe<sub>2</sub>O<sub>4</sub> compounds have been extensively investigated. XRD, Raman, SEM-EDAX and AFM techniques have been used for structural analysis; Absorption technique has been used for optical properties; Vibrating sample magnetometer (VSM) techniques have been used for magnetic properties. XRD analysis of the growth films revealed that Co:Fe<sub>2</sub>O<sub>3</sub> film has monoclinic, Co<sub>x</sub>Zn<sub>1-x</sub>Fe<sub>2</sub>O<sub>4</sub> films have cubic polycrystalline structures. Gas sensors can be made from various materials depending on the purposes they serve. Regardless type of gas sensor, general requirements for a reliable gas sensor is high sensitivity, fast response, and good selectivity. It was found that Co:Fe<sub>2</sub>O<sub>3</sub> and Co<sub>x</sub>Zn<sub>1-x</sub>Fe<sub>2</sub>O<sub>4</sub> thin films operating at 200°C temperature could detect H<sub>2</sub> at 100 ppm, 500 ppm and 1000 ppm concentration and at 600 s time with very high selectivity and sensitivity, with better stability.

**KEYWORDS:** Gas sensor; Co:Fe<sub>2</sub>O<sub>3</sub>; Chemical spray pyrolysis (CSP); Thin film

### I. INTRODUCTION

Interest in detecting and determining concentrations of toxic and flammable gases has constantly been on the increase in recent years due to increase of industrialization. Metaloxide gas sensors are among most important devices to detect a large variety of gases.  $\alpha$ -Fe<sub>2</sub>O<sub>3</sub>, an environmental friendly semiconductor (e.g. = 2.1 eV), is the most stable iron oxide under ambient atmosphere and because of its low cost, high stability, high resistance to corrosion, and its environmentally friendly properties is one of the most important metal oxides for gas sensing applications[1].

In terms of gas sensor,  $\alpha$ -Fe<sub>2</sub>O<sub>3</sub>-based sensors is widely applicable for the detection of various gases such as H<sub>2</sub>, O<sub>2</sub>, CO, H<sub>2</sub>O etc. However, several obstacles have to be overcome for its future application. For example, the working temperatures are still high, and the recovery time is too long. These shortcomings can be partly avoided or improved by depositing noble metals, by composing with other semiconductors, and, most importantly, by introducing newly developed nanostructured  $\alpha$ -Fe<sub>2</sub>O<sub>3</sub> to the sensors. Pure  $\alpha$ -Fe<sub>2</sub>O<sub>3</sub> gas sensors are very cheap and are show higher sensitivity to ethanol and acetone, however they suffer from lack of selectivity and sometime low sensitivity.



# International Journal of Advanced Research in Electrical, Electronics and Instrumentation Engineering

(An ISO 3297: 2007 Certified Organization)

Website: [www.ijareeie.com](http://www.ijareeie.com)

Vol. 6, Issue 7, July 2017

The synthesis and functionalism of low dimensional nanostructured ferric oxide ( $\alpha$ -  $\text{Fe}_2\text{O}_3$ ) has fascinated the researchers due to their significant potential applications [2]. Various chemical pollutants have been released in high quantities into the atmosphere as a result of human activities and have generated environmental risks one of the critical factors that contribute to global warming, climate changes, and harm to human health. In order to monitor air pollution on a large scale, inexpensive, reliable and easy to use gas sensors are needed. The electrical resistance of semiconductor oxides, such as  $\text{SnO}_2$ ,  $\text{ZnO}$ ,  $\text{TeO}_2$ ,  $\text{WO}_3$  and  $\text{Fe}_2\text{O}_3$ , has a strong dependence on the concentration of surrounding gases. According to this principle, these oxides are commercially designed as chemical sensors to detect toxic gases such as LPG, and  $\text{NO}_2$ [3,4]. Ferric oxide is considered to be the most promising highly sensing materials of sensors due to the temperature dependent surface morphology and photo catalytic activity [5]. For gas sensing applications, the materials having lower density and higher active surface area are challenging for the fabrication of sensors.

## II. EXPERIMENTAL DETAILS

The technique of CSP without the requirement of vacuum is a method that can be preferred in the industry, in order to allow the production of large size films in both cheap. However, there are some disadvantages of films made with this technique, such as their thickness being not uniform and the size of the film-forming atoms being limited and the film in chemical solution to be grown must be homogeneous. Many parameters such as substrate, substrate temperature, the salts, solvent type, molarity and deposition time have carefully been chosen to obtain the best growth condition in this technique. The salts given in Table 1 were prepared as 0.1 molar solution in deionized water. The substrate was sprayed with argon gas onto a substrate heated to  $320^\circ\text{C}$  at a distance of 30 cm.

Film	Used Chemical Salt	Solution Molar Ratio	Substrate Temperature ( $^\circ\text{C}$ )	Carrier gas	Grown Time (min)
$\text{Co}_x\text{Zn}_{1-x}\text{Fe}_2\text{O}_4$	$\text{FeCl}_3 \cdot 6\text{H}_2\text{O} + \text{FeCl}_2 \cdot 4\text{H}_2\text{O} + \text{NaOH} + \text{Co}(\text{NO}_3)_2 \cdot 6\text{H}_2\text{O} + \text{Zn}(\text{NO}_3)_2 \cdot 6\text{H}_2\text{O}$	1:2:0.25:0.1:0.01	320	Argon	35
$\text{Co}:\text{Fe}_2\text{O}_3$	$\text{FeCl}_3 \cdot 6\text{H}_2\text{O} + \text{FeCl}_2 \cdot 4\text{H}_2\text{O} + \text{NaOH} + \text{Co}(\text{NO}_3)_2 \cdot 6\text{H}_2\text{O}$	1:2:0.25:0.1	320	Argon	35

Table 1: Experimental details of the  $\text{Co}:\text{Fe}_2\text{O}_3$  and  $\text{Co}_x\text{Zn}_{1-x}\text{Fe}_2\text{O}_4$  thin films grown by chemical spray pyrolysis technique.

## III. RESULTS AND DISCUSSION

The structural, optical and magnetic properties of  $\text{Co}:\text{Fe}_2\text{O}_3$  and  $\text{Co}_x\text{Zn}_{1-x}\text{Fe}_2\text{O}_4$  compounds have been extensively investigated. XRD, Raman, SEM-EDAX and AFM techniques have been used for structural analysis; Absorption technique has been used for optical properties; Vibrating sample magnetometer (VSM) techniques have been used for magnetic properties and I-V technique has been used for response of gas sensor Figure 1 and Table 2 [6].



# International Journal of Advanced Research in Electrical, Electronics and Instrumentation Engineering

(An ISO 3297: 2007 Certified Organization)

Website: [www.ijareeie.com](http://www.ijareeie.com)

Vol. 6, Issue 7, July 2017

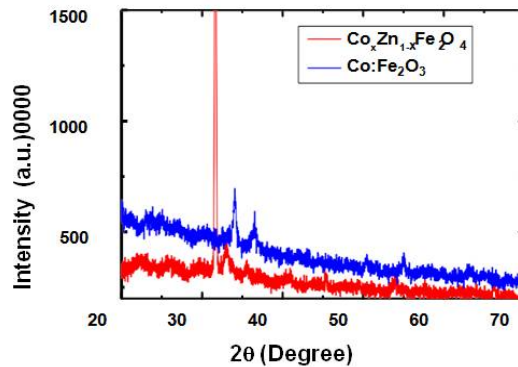


Figure 1: XRD patterns of Co:Fe<sub>2</sub>O<sub>3</sub> and Co<sub>x</sub>Zn<sub>1-x</sub>Fe<sub>2</sub>O<sub>4</sub> thin films.

Literature 2θ°	Experimental 2θ°	(hkl)	Fwhm	Lattice constant	d (Å)	Crystal system	Chemical formula	Reference Code
34,84	34,11	-213	0.34	a=12,97 b=10,21 c= 8,44	2,57	Monoclinic	Fe <sub>2</sub> O <sub>3</sub>	00-016-0653
36,52	36,81	23	0.17	a=12,97 b=10,21 c= 8,44	2,45	Monoclinic	Fe <sub>2</sub> O <sub>3</sub>	00-016-0653
50,46	50,43	-631	0.11	a=12,97 b=10,21 c= 8,44	1,80	Monoclinic	Fe <sub>2</sub> O <sub>3</sub>	00-016-0653
55,08	55,10	352	0.09	a=12,97 b=10,21 c= 8,44	1,66	Monoclinic	Fe <sub>2</sub> O <sub>3</sub>	00-016-0653

Table 2: Structural properties obtained from XRD patterns of Co:Fe<sub>2</sub>O<sub>3</sub> thin film.

Experimental 2θ°	(hkl)	Fwhm	d (Å)	Crystal system	Chemical formula	Lattice constant	Reference Code
31,71	220	0,155	2,81	Cubic	ZnCo <sub>2</sub> O <sub>4</sub>	a= b=c=8,42	00-001-1149
32,97	222	0,035	2,71	Rhombohedral	Fe <sub>2</sub> O <sub>3</sub>	a=b=5,03 c=13,74	01-079-1741
35,45	311	0,11	2,53	Cubic	(Zn <sub>0,54</sub> Fe <sub>0,46</sub> ) Fe <sub>2</sub> O <sub>4</sub>	a=b=c=8,42	01-086-0509
66,29	442	0,090	1,41	Cubic	(Zn <sub>0,54</sub> Fe <sub>0,46</sub> ) Fe <sub>2</sub> O <sub>4</sub>	a=b=c= 8,42	01-086-0509

Table 3: Structural properties obtained from XRD patterns of Co<sub>x</sub>Zn<sub>1-x</sub>Fe<sub>2</sub>O<sub>4</sub> thin film.

## International Journal of Advanced Research in Electrical, Electronics and Instrumentation Engineering

(An ISO 3297: 2007 Certified Organization)

Website: [www.ijareeie.com](http://www.ijareeie.com)

Vol. 6, Issue 7, July 2017

XRD analysis of the growth films revealed that  $\text{Co:Fe}_2\text{O}_3$  film has monoclinic and  $\text{Co}_x\text{Zn}_{1-x}\text{Fe}_2\text{O}_4$  films have heavily cubic polycrystalline structures. XRD results indicated that cobalt successfully replaced iron in the host lattice. The peak positions shifted to higher angles due to lower ionic radius of cobalt as compared to that of iron Table 3.

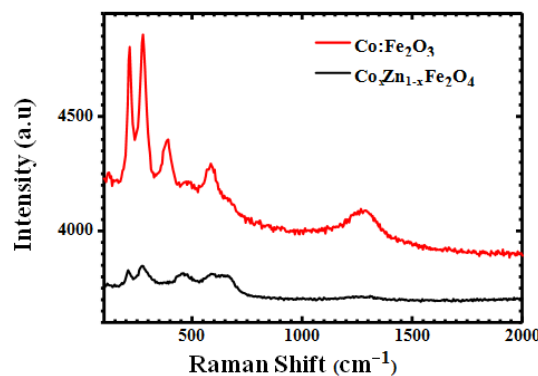


**Figure 2:** Raman scattering intensities are shown as a function of wavenumber for  $\text{Co:Fe}_2\text{O}_3$  and  $\text{Co}_x\text{Zn}_{1-x}\text{Fe}_2\text{O}_4$  thin films.

Figure shows the Raman shift of the stretching vibration mode of  $\text{Co:Fe}_2\text{O}_3$  films are seen. There are Raman active states of the hematite phase that these peaks are relatively narrow and severe. In the  $\text{Co}_x\text{Zn}_{1-x}\text{Fe}_2\text{O}_4$  compound, the peak of the Raman shift peaks belonging to the hematite phase falls (Figure 2). In addition, the peaks showing the ramping changes of the stretching vibration mode of the  $\text{Co}_x\text{Zn}_{1-x}\text{Fe}_2\text{O}_4$  film is due to the presence of multiple phases due to polycrystalline crystal structure and also impurity, oxygen vacancies, interstitial ion [7-11] (Table 4).

Compounds	Raman Shift ( $\text{cm}^{-1}$ )	Mod
$\text{Fe}_2\text{O}_3$	217; 277; 388; 584; 1284; 2891;	Hematit; [(A1g) 225], [(A1g) 229], [(Eg) 247], [(Eg) 249], [(Eg) 295], [(Eg) 302], [(Eg) 412], [(A1g) 500], [(Eg) 615], [(Eu) 660 LO], [(a- $\text{Fe}_2\text{O}_3$ ) 1320] [12-14]
$\text{Co}_x\text{Zn}_{1-x}\text{Fe}_2\text{O}_4$	117; 145; 206; 273; 464; 591; 656; 1286	Hematit[(A1g) 229], [(Eg) 247], [(A1g) 225] [A1g ( $\text{Co}_x\text{Zn}_{1-x}\text{Fe}_2\text{O}_4$ ) (464-656)], [(a- $\text{Fe}_2\text{O}_3$ ) 1320] [15]

**Table 4:** Raman shift and modes of  $\text{Co: Fe}_2\text{O}_3$  and  $\text{Co}_x\text{Zn}_{1-x}\text{Fe}_2\text{O}_4$  thin films.

# International Journal of Advanced Research in Electrical, Electronics and Instrumentation Engineering

(An ISO 3297: 2007 Certified Organization)

Website: [www.ijareeie.com](http://www.ijareeie.com)

Vol. 6, Issue 7, July 2017

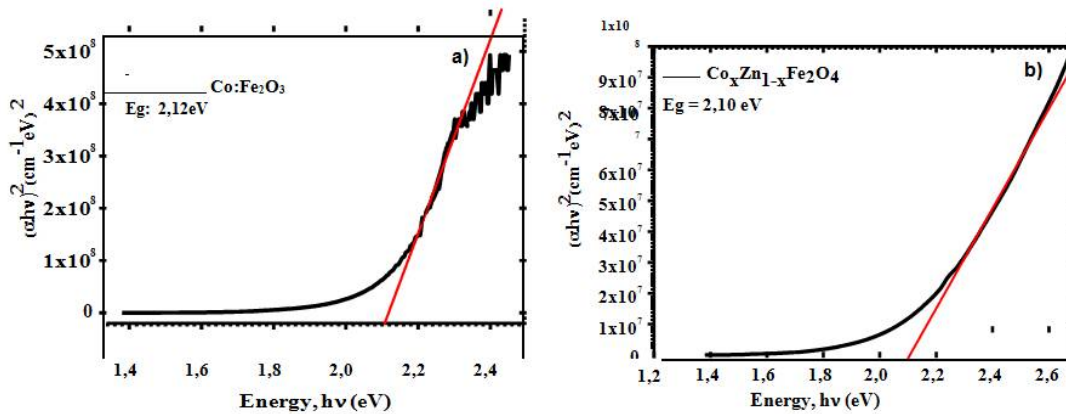


Figure 3: Plot of  $(\alpha hv)^2$  (cm<sup>-1</sup> eV<sup>2</sup>) vs. photon energy  $h\nu$  (eV) of a) Co: Fe<sub>2</sub>O<sub>3</sub> b) Co<sub>x</sub>Zn<sub>1-x</sub>Fe<sub>2</sub>O<sub>4</sub> thin films.

In Figure 3 the value of the energy of the band gap is calculated to be 2.10 eV, 2.12 eV with the fit drawn on the energy graph against the  $(\alpha hv)^2$  (cm<sup>-1</sup> eV<sup>2</sup>) of the Co: Fe<sub>2</sub>O<sub>3</sub>, Co<sub>x</sub>Zn<sub>1-x</sub>Fe<sub>2</sub>O<sub>4</sub> thin films grown by CSP technique, respectively. As Co<sub>x</sub>Zn<sub>1-x</sub>Fe<sub>2</sub>O<sub>4</sub> thin film gives absorption at smaller wave lengths, it shifts at larger wave length as a result of doping. We can say that the holes in the valence band of the p-type semiconducting material are compensated by the donor type defects and impurities. This may mean that the energy gap of Co<sub>x</sub>Zn<sub>1-x</sub>Fe<sub>2</sub>O<sub>4</sub> is larger than Co: Fe<sub>2</sub>O<sub>3</sub> band gap.

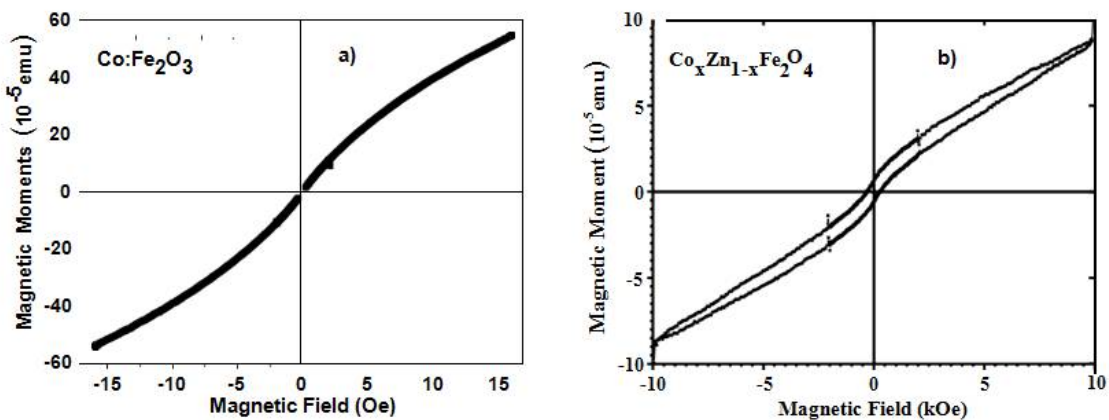


Figure 4: M-H curves for a) Co: Fe<sub>2</sub>O<sub>3</sub> and b) Co<sub>x</sub>Zn<sub>1-x</sub>Fe<sub>2</sub>O<sub>4</sub> thin films.

In Figure 4 the magnetic hysteresis curve of the Co:Fe<sub>2</sub>O<sub>3</sub> thin film is observed to be relatively narrow. The saturation magnetic torque value is  $55.5 \cdot 10^{-5}$  emu, which corresponds to a value of 15.94 Oe. In addition, the coercive force is -0.008 Oe and the remanence magnetic moment is 0.063. It has an emu value of  $10^{-5}$ . In these values, it has been determined that Co:Fe<sub>2</sub>O<sub>3</sub> has a soft magnetic property.



## International Journal of Advanced Research in Electrical, Electronics and Instrumentation Engineering

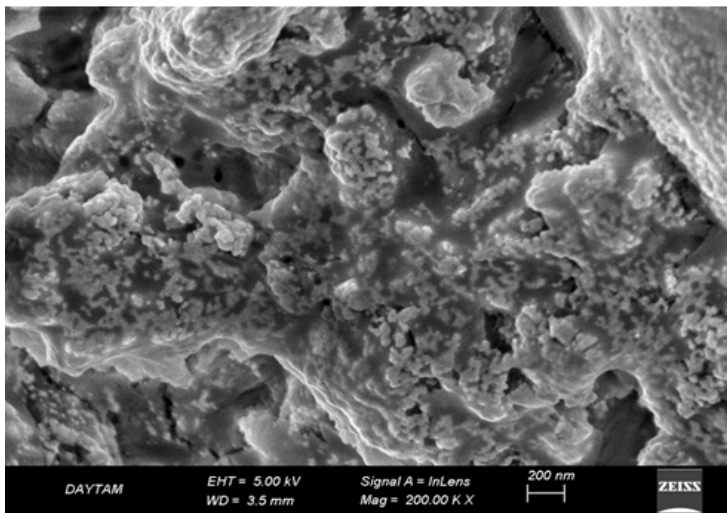
(An ISO 3297: 2007 Certified Organization)

Website: [www.ijareeie.com](http://www.ijareeie.com)

Vol. 6, Issue 7, July 2017

Among the various phases of iron oxide,  $Fe_2O_3$  is the most stable form of iron oxide that shows antiferromagnetic behaviour. Doping of different metal ions in  $\alpha-Fe_2O_3$  will lead to its new technological and industrial applications and enhancement of its performance in existing applications. Cobalt doped  $Fe_2O_3$  thin films showed ferromagnetic behavior because of the presence of uncompensated spins arising from cobalt doping [11-15].

In Figure 4 the magnetic hysteresis curve of the Co:  $Fe_2O_3$  thin film is observed to be relatively narrow. The saturation magnetic torque value is  $55.5 \cdot 10^{-5} \text{ emu}$ , which corresponds to a value of 15.94 Oe. In addition, the coercive force is - 0.008 Oe and the remanence magnetic moment is 0.063. It has an emu value of  $10^{-5}$ . When the hysteresis curve is taken into consideration, it can be said that the material exhibits hard magnetism and is difficult to demagnetize due to the Zn doping. The nonmagnetic property of the Zn element affects the magnetic moment of the Zn doping which leads to pinning spin and makes the domain motion difficult.



Element	Mass %	Atomic%
Fe	35.84	18.72
O	40.1	64.68
Zn	5.33	1.91
Cl	5.27	0.37
Au	3.02	0.47
Co	4.44	2.32

Figure 5: FE-SEM images and EDX analysis table of  $Co_xZn_{1-x}Fe_2O_4$  thin film.

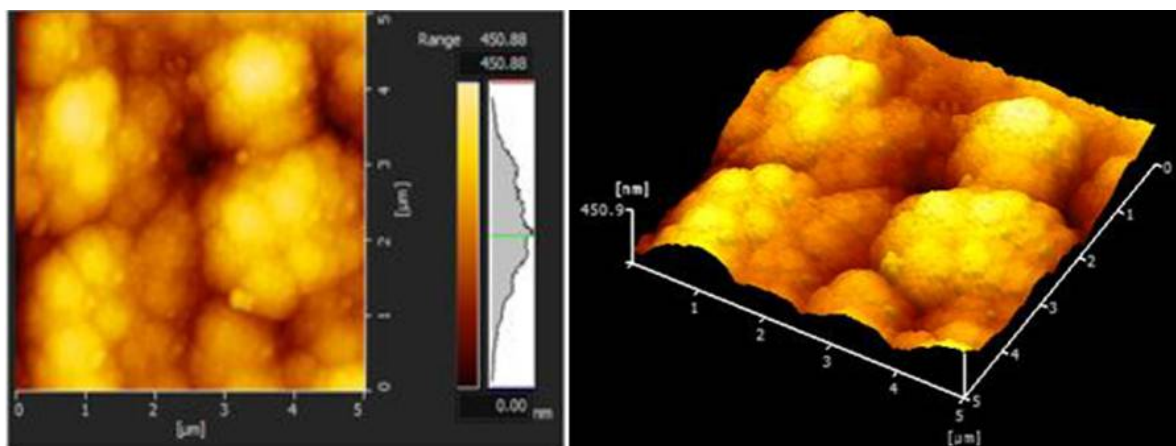


Figure 6: Two-dimensional and three-dimensional AFM images of the  $Co_xZn_{1-x}Fe_2O_3$  thin film grown on glass substrates. The  $Co_xZn_{1-x}Fe_2O_3$  films line roughness value is about 49 nm.

# International Journal of Advanced Research in Electrical, Electronics and Instrumentation Engineering

(An ISO 3297: 2007 Certified Organization)

Website: [www.ijareeie.com](http://www.ijareeie.com)

Vol. 6, Issue 7, July 2017

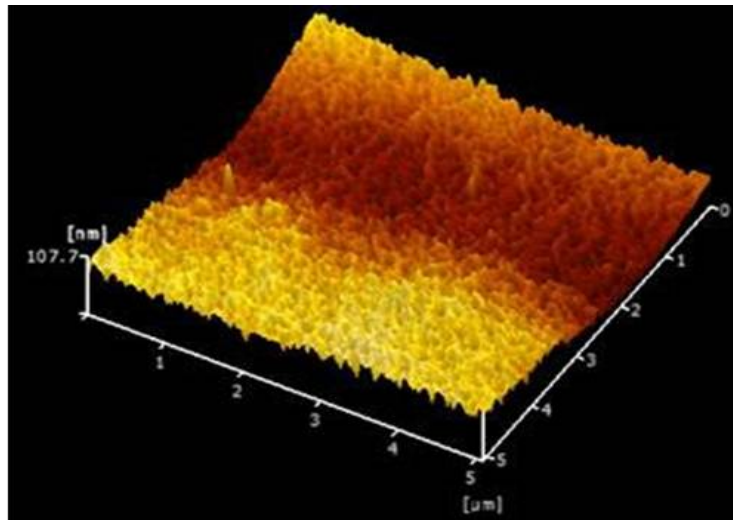
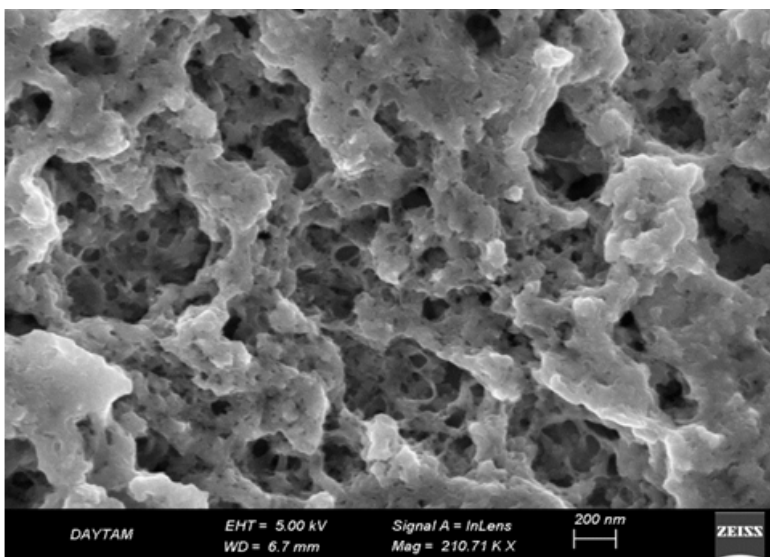


Figure7: AFM images of the  $\text{Co}_x\text{Zn}_{1-x}\text{Fe}_2\text{O}_4$  thin film grown on glass substrates (5 minutes grown). The  $\text{Co}_x\text{Zn}_{1-x}\text{Fe}_2\text{O}_4$  films line roughness value is about 6.9 nm.

The nano-pores found in the FE-SEM image of the  $\text{Co}_x\text{Zn}_{1-x}\text{Fe}_2\text{O}_4$  (5 minutes grown) structure show a sharp-pointed sequence with a clearly noticeable structure. The thickened residues formed concentrated areas due to gravity. When the structure is thin, the interactions vary in thickness. The structure is arranged very regularly and is clearly observed. Thickness of the grain at the surface of the crystal is much larger than that of the crystal. The  $\text{Co}_x\text{Zn}_{1-x}\text{Fe}_2\text{O}_4$  films roughness value is about 49 nm (Figures 5 to 7).



Element	Mass %	Atomic%
Fe	47.64	26.87
O	33.96	56.01
Cl	14.53	12.91
Co	7.87	4.2

Figure 8: FE-SEM images and EDX analysis table of Co:  $\text{Fe}_2\text{O}_3$  thin film.

## International Journal of Advanced Research in Electrical, Electronics and Instrumentation Engineering

(An ISO 3297: 2007 Certified Organization)

Website: [www.ijareeie.com](http://www.ijareeie.com)

Vol. 6, Issue 7, July 2017

The Co: Fe<sub>2</sub>O<sub>3</sub> compound appears to have a nanoporous structure in the SEM image taken from an area of 200 nm at 210,000 magnifications taken from the inlens detector. This literature study suggests that it is suitable for supercapacitor and gas sensor application [7-10]. Cl element in the EDX results are due to salts used in the solution and the Au element in the EDX results is due to the coating made to clarify the image during FE-SEM measurement. We can say the Cl element remained unvaporized due to the low substrate temperature (Figure 8).

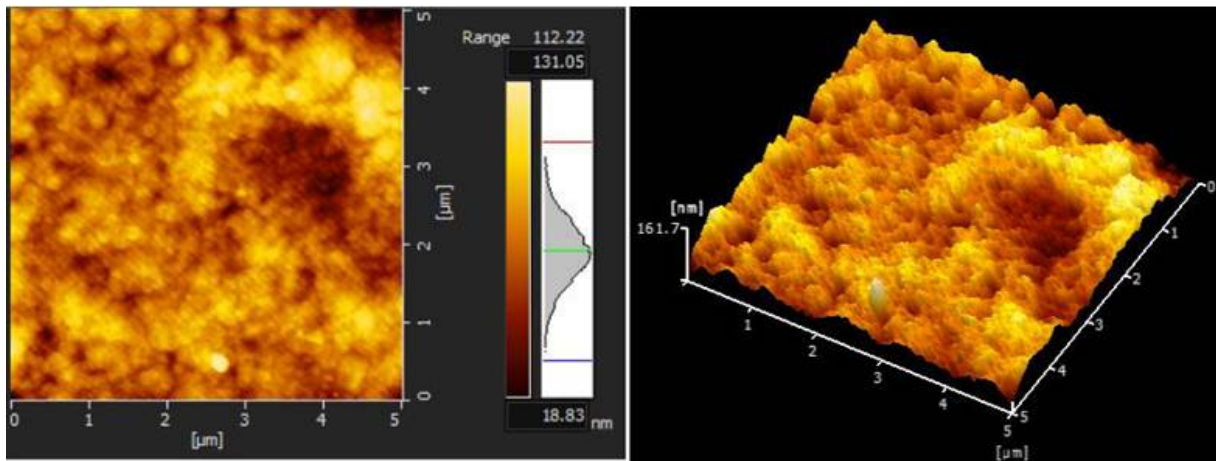
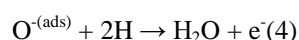
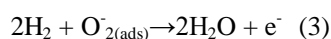
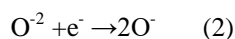
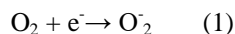


**Figure 9: Two-dimensional and three-dimensional AFM images of the Co: Fe<sub>2</sub>O<sub>3</sub> thin film grown on glass substrates. The Co: Fe<sub>2</sub>O<sub>3</sub> films line roughness value is about 10 nm.**

In Figure 9 the two-dimensional and three-dimensional AFM images obtained for the Co: Fe<sub>2</sub>O<sub>3</sub> film showed that the particles in the structure showed a more sharp image. There are pits and hills almost everywhere in the landscape resembling craters. The roughness value is about 10 nm. The variability of the colors tone indicates that the height difference in the topography is great. It is possible to say that the surface consists mostly of hills and pits.

When we get the gas sensor measure we see that Co: Fe<sub>2</sub>O<sub>3</sub> and Co<sub>x</sub>Zn<sub>1-x</sub>Fe<sub>2</sub>O<sub>4</sub> is the n type semiconductor. Because of the electrons that emerge as a result of the reaction increase the carrier concentration. Thus resistance is reduced.





## International Journal of Advanced Research in Electrical, Electronics and Instrumentation Engineering

(An ISO 3297: 2007 Certified Organization)

Website: [www.ijareeie.com](http://www.ijareeie.com)

Vol. 6, Issue 7, July 2017

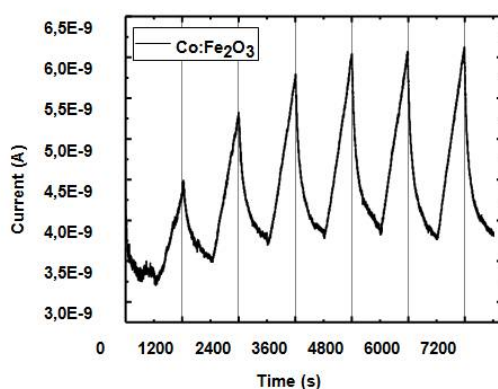


**Figure 10: Sensor Response of Co: Fe<sub>2</sub>O<sub>3</sub> thin film deposited by using Chemical Spray Pyrolysis (CSP) technique towards H<sub>2</sub> target gases for different concentrations (100 ppm, 500 ppm, 1000 ppm) at 200°C temperature.**

In Figure 10 Co: Fe<sub>2</sub>O<sub>3</sub> shows the time-dependent change in the response of the thin film to hydrogen gas, and the measurement is periodically 600 s nitrogen and 600 s hydrogen gas at 200°C. This measurement was made to evaluate the response of the thin film to hydrogen gas, and the reaction of the film to hydrogen gas was found to be very high. During the measurement periodically 600 s nitrogen and 600 s hydrogen gas were supplied to the system at 200°C temperature. The film, which did not react to hydrogen gas at room temperature, reacted at a temperature of 200°C. Nitrogen was used as the sweeping gas. In the first 600 s 500 ppm nitrogen swept system, 100 ppm hydrogen gas was then supplied and the amount of current drawn by the system increased. When the nitrogen is swept in again, the current drawn is reduced and receded to the previous level. 500 ppm for 600 s in the second cycle, 1000 ppm for 600 s in the third cycle and the current value increased with the hydrogen value. The same gauge is repeated after 24 hours and the same result was obtained. This material is a promising material for gas sensor application.

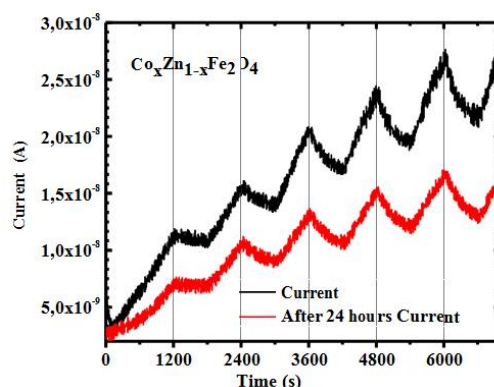


**Figure 11: Sensor Response of Co<sub>x</sub>Zn<sub>1-x</sub>Fe<sub>2</sub>O<sub>4</sub> thin film deposited by using CSP technique towards H<sub>2</sub> target gases for different concentrations (100 ppm, 500 ppm, 1000 ppm) at 200°C temperature.**



# International Journal of Advanced Research in Electrical, Electronics and Instrumentation Engineering

(An ISO 3297: 2007 Certified Organization)

Website: [www.ijareeie.com](http://www.ijareeie.com)

Vol. 6, Issue 7, July 2017

As mentioned earlier, there is a gas sensor application of the  $\text{Co}_x\text{Zn}_{1-x}\text{Fe}_2\text{O}_4$  compound in the literature. In addition to being used for spintronic applications due to its magnetic properties, it is available in gas sensor applications due to the large surface area of the material with a thickness of 100 nm and above [6]. In Figure 11,  $\text{Co}_x\text{Zn}_{1-x}\text{Fe}_2\text{O}_4$  shows the time-dependent change in the response of the thin film to hydrogen gas, and the measurement is periodically 600 s nitrogen and 600 s hydrogen gas at 200°C. This measurement was made to evaluate the response of the thin film to hydrogen gas, and the reaction of the film to hydrogen gas was found to be very high. During the measurement periodically 600 s nitrogen and 600 s hydrogen gas were supplied to the system at 200°C temperature. The film, which did not react to hydrogen gas at room temperature, reacted at a temperature of 200°C. Nitrogen was used as the sweeping gas. In the first 600 s 500 ppm nitrogen swept system, 100 ppm hydrogen gas was then supplied and the amount of current drawn by the system increased. When the nitrogen is swept in again, the current drawn is reduced, but not receded to the previous level. This means that some of the hydrogen remains in the structure. 500 ppm for 600 s in the second cycle, 1000 ppm for 600 s in the third cycle and the current value increased with the hydrogen value. The same gauge is repeated after 24 hours, indicating that hydrogen is held at a lower level, which means that the hydrogen is stored in the structure, during which the hydrogen is separated from the structure in very small amounts. This material is a promising material for gas sensor application as well as promising hydrogen storage applications. 100; R sensors response, I; first current, I finally current. According to calculations made, Table 5 gives the responses of the gas sensors.

Time	600.s	1200.s	1800.s
Compound	(100 ppm)	(500 ppm)	(1000 ppm)
Co: $\text{Fe}_2\text{O}_3$	23.33%	35%	38%
$\text{Co}_x\text{Zn}_{1-x}\text{Fe}_2\text{O}_4$	11%	18.35%	22%
$\text{Co}_x\text{Zn}_{1-x}\text{Fe}_2\text{O}_4$ After 24 hour	10.59%	22%	27%

Table 5:  $\text{Co}_x\text{Zn}_{1-x}\text{Fe}_2\text{O}_4$  and Co:  $\text{Fe}_2\text{O}_3$  gas sensors response depends of gas flow rate.

### III. CONCLUSION

This material is a promising material for gas sensor application as well as promising hydrogen storage applications. When we consider the magnetization situation, the hardest magnetization property is  $\text{Co}_x\text{Zn}_{1-x}\text{Fe}_2\text{O}_4$  film, the softest magnetization feature is Co:  $\text{Fe}_2\text{O}_3$  film. It can be said here that Zn, which has no magnetic property, causes pinning which make defects in the structure difficult to move the domains. As can be seen from the VSM results, these materials can also be used for spintronic applications.

### REFERENCES

1. Mirzaei A, Hashemi B, et al. A-  $\text{Fe}_2\text{O}_3$  based nanomaterials as gas sensors. J Mater Sci: Mater Electron 2016; 27:3109–3144.
2. Mukherjee S, Pal AK, EPR Studies on sol–gel derived  $\text{Fe}_2\text{O}_3$  nanocrystals in  $\text{SiO}_2$  matrix, Proceedings of the First International Symposium. Solid State Physics 2003; 23: 205–206.
3. Sonker RK, Yadav BC, Chemical Route Deposited  $\text{SnO}_2$ ,  $\text{SnO}_2$ -Pt and  $\text{SnO}_2$ -Pd Thin Films for LPG Detection. Adv. Sci. Lett., 2014; 20: 1023-1027.
4. Sonker RK, Yadav BC, Synthesis of ZnO nanopeels and its application as  $\text{NO}_2$  gas sensor. Materials Letters 2015; 152: 189–191.



ISSN (Print) : 2320 – 3765  
ISSN (Online): 2278 – 8875

## International Journal of Advanced Research in Electrical, Electronics and Instrumentation Engineering

(An ISO 3297: 2007 Certified Organization)

Website: [www.ijareeie.com](http://www.ijareeie.com)

Vol. 6, Issue 7, July 2017

5. Chaudhari NK, Yu JS, Size control synthesis of uniform  $\beta$ -FeOOH to high coercive field porous magnetic  $\alpha$ -Fe<sub>2</sub>O<sub>3</sub> nanorods. J. Phys. Chemistry C 2008; 112: 19957–19962.
6. Panda J, Nath TK, Low temperature junction magnetoresistance properties of Co<sub>0.65</sub>Zn<sub>0.35</sub>Fe<sub>2</sub>O<sub>4</sub>/SiO<sub>2</sub>/p-Si magnetic diode like heterostructure for spin-electronics. Thin Solid Films 2016; 601: 111–118.
7. Ho MY, Khiew PS, Shamsuddin, Nano Fe<sub>3</sub>O<sub>4</sub>-activated carbon composites for aqueous supercapacitors. Sains Malaysiana 2014; 43: 885–894.
8. Lokhande CD, Dubal DB, Metal oxide thin film based supercapacitors. Curr Appl Phys 2011; 11: 255–270.
9. Ilgeun O, Kim M, Controlling hydrazine reduction to deposit iron oxides on oxidized activated carbon for supercapacitor application. Energy 2015; 86: 292–299.
10. Pawar NK, Kajale GH, Nanostructured Fe<sub>2</sub>O<sub>3</sub> thick film as an ethanol sensor. International Journal on Smart Sensing and Intelligent Systems 2012; 5: 2.
11. Aseya A, Sidra B, Magnetic Properties of Co-doped Fe<sub>2</sub>O<sub>3</sub> Thin Films. Materials Today: Proceedins 2015; 2: 5674 – 5678.
12. Chamritskii I, Burns G, Infrared and Raman-active phonons of magnetite, maghemite, and hematite: a computer simulation and spectroscopic study. J Phys Chem B 2005; 109: 4965–4968.
13. Bersani D, Lottici P, Micro-Raman investigation of iron oxide films and powders produced by sol-gel syntheses. J Raman Spectrosc 1999; 30: 355–360.
14. Jubb AM, Allen HC, Vibrational spectroscopic characterization of hematite, maghemite, and magnetite thin films produced by vapor deposition. Applied materials and interface 2010; 2: 2804–2812.
15. Rahimi M, Kameli P, The effect of zinc doping on the structural and magnetic properties of Ni<sub>x</sub>Zn<sub>1-x</sub>Fe<sub>2</sub>O<sub>4</sub>. J Mater Sci 2013; 48: 2969–2976.